MULTIDISCIPLINARY SCIENCE JOURNAL

RESEARCH ARTICLE
Published Online: October 19, 2023
https://doi.org/10.31893/multiscience.2024053

4G based SAR analysis for anatomically based human head model using mobile phone antenna

Amol Sonawane[a] | **Dattatraya Bormane**[b]

[a]Electronics Engineering Department, AISSMS's Institute of Information and Technology, India.
[b]Electronics Engineering Department, AISSMS's College of Engineering, India.

Abstract Mobile phone handsets utilized by individuals of all ages been heavily grows popular as a wireless communication device. Every mobile phone produces electromagnetic radiation at radio frequencies (RF). The specific absorption rate is used to calculate how much of this energy is absorbed by the human skull. Standard guidelines state that sold phones must fall below a specified SAR. This paper aims to evaluate the Specific Absorption Rate (SAR) and E-field strength for mobile phone radiation exposure on a head model who is 40 years old and a 5-year-old child. The human skull is represented in this model as a six-layered sphere made up of the brain, CSF, dura, bone, fat, and skin. Various layers of the head's SAR distribution have been measured as an impact of radiation from mobile phones exposure using the 1800 MHz frequency. Earlier research were used to consider the dielectric properties of tissue layers. The human head and mobile phone antenna is modelled in this research using ANSYS HFSS. A hand-held mobile phone's dipole antenna type is considered for RF exposure. It is seen how EM absorption in various tissue layers for both adults as well as child head. SAR comparisons between the adult and child head reveal that the child head absorbs greater power due to the distinctive layerwise head shape, conductivity, permittivity, and permeability of the two head models. Excess EM absorption may have negative physiologic implications for human health specifically impact on child physical and mental health.

Keywords: specific absorption rate, mobile phone model, half wave dipole antenna, electromagnetic radiation

1. Introduction

Some studies have examined the negative biological impacts on human health as a result of the potential effects of electromagnetic (EM) fields on human tissues and body parts. There are safety concerns regarding the effect of the mobile antenna on the head when using mobile phones for wireless communication that function near the human head. The features of an antenna, such as the radiation pattern, are influenced by the user's body, particularly the head. An internal EM field is produced in a biological system when it is subjected to microwave radiation. More than half of the antenna's emitted power is reportedly absorbed by the tissues of the cranium, according to experimental investigations (Sonawane and Bormane 2020; Means and Chan 2001).

The rate at which RF energy is absorbed by the body when exposed to an electromagnetic field is measured as the specific absorption rate. The rate of absorption and how it is distributed within an organism depends on a number of variables, including the antenna's shape, distance from the source, geometry, and orientation, as well as the dielectric composition of the irradiated tissue (i.e., its capacity to conduct electricity) (Arima and Uno 2012). For example, bone absorbs less energy than muscle because it contains less water. Additionally, the age and amount of SAR produced in the cranium are known to be related (Abdalla and Teoh 2005). Researchers are looking at the impacts of these tissues after intense radiation from wireless devices, specifically mobile phones directed at the head, the most vulnerable part of the human body. The electrical parameters of the model tissues at various frequencies were considered (Fernandez-Rodriguez et al 2015).

There are numerous ways to evaluate SAR, including two well-known methods: either physical measurements or simulation calculation measurements can be used to assess the electromagnetic interaction between a cell phone and a human body.

In the aforementioned study, the High Frequency Structure Simulator software simulation, which uses the Finite Difference Time Domain approach, produces an SAR for a spherical human head. A six-layered head model made up of the brain, CSF, dura, bone, fat and skin is used to show how the head is affected by radiative functioning of the antenna. For the 5-year-old child head and the 40-year-old adult head, SAR was evaluated using an HFSS-based HW dipole antenna, and human model head simulations were used to perform the analysis. A six-layer model of the human skull was created using

 Received: August 04, 2023 | Accepted: September 23, 2023

HFSS software, and the HW dipole antennas were placed 5 mm apart. At 1800 MHz, two scenarios were simulated, one using a six-layered child head with a dipole antenna and the other using a six-layered adult head with a dipole antenna. The findings revealed that the head's average 10 g SAR values were higher than the ICNIRP safety requirements (ICNIRP 1998; Means and Chan 2001). The standard SAR values taken in the extremities and other tissues, such as the brain, are shown in Table 1.

Table 1 Standard SAR limits.

	ICNIRP 1998	FCC OET B-65/2001	IEEE C95.1/2005
Extremities	4 W/kg over 10 g	4 W/kg over 10 g	4 W/kg over 10 g
Other tissues	2 W/kg over 10 g	1.6 W/kg over 1 g	2 W/kg over 10 g

The averaged SAR values for the adult and child heads reveal that SAR is higher in children because their heads are smaller and have different electrical properties than adult heads. Figure 1 shows physical and simulation-based SAR assessment methods.

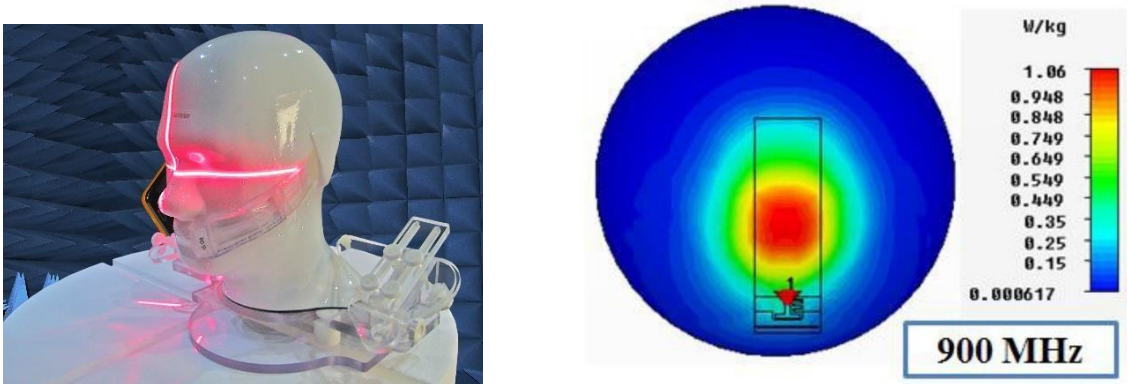

(A) (B)

Figure 1 SAR assessment methods (A) Physical measurements, http://www.indexsar.com (B) Simulation measurements.

2. Methodology

2.1. Specific Absorption Rate

Whenever there is an interaction between human tissue and electromagnetic waves, tissue absorbs EM waves. A certain absorption rate can be used to characterize how electromagnetic fields interact with biological tissues called the specific absorption rate (SAR). This acts as an index that gauges the intensity of the RF EM field in the brain that a mobile phone emits under the worst circumstances when it is working at full power. Watts per kilogram (W/kg) is its unit. To prevent health risks, governments have established limits for the highest SAR that should not be surpassed. In the US and European countries, this limit is established at an average of 1.6 W/kg and 2 W/kg over 1 g and 10 g of tissue, respectively. The following equation describes the SAR:

$$SAR = \frac{\sigma |E|^2}{2\rho} \qquad (1)$$

where σ in Siemens per meter indicates electrical conductivity and ρ in kilograms per cubic meter shows tissue density. From the estimated local fields and tissue characteristics, SAR is determined as a function of location. The absorbed power is calculated as the integral of the SAR across a tissue volume with a certain specific mass. For a particular tissue density, this is commonly represented in terms of mW/g or mW/cm3 averaged over 1 g of tissue.

3. Models and Materials

3.1. Antenna Model

The following geometrical properties of an HW dipole radiator are exposed to the head model: the dipole length is 79.44 mm with a spacing of 0.3972 mm, while the radius is 0.167 mm. Models of the antenna's edges depicted them as ideal electrical conductors. The antenna's operating frequency is 1800 MHz. The radiation boundary in our case was a cube. The substance was designated as vacuum at the radiation boundary. Table 2 shows the antenna design parameters considered for the HW dipole antenna. Table 2 shows a summary of the antenna parameters.

To enhance the results, simulation was utilized to examine performance factors such as gain, radiation pattern, reflectance, and VSWR. The suggested HW dipole antenna has a bandwidth of 424.3 Megahertz, a return loss of -20.7710 dB, and a VSWR of 1.5901 dB. Figure 2 shows an 1800 MHz HW dipole antenna, and Figure 3 shows the antenna design flow chart for the simulation. Figures 4, 5, and 6 show the bandwidth and return loss curve, VSWR plot and 3D gain radiation pattern, respectively, for an HW dipole antenna.

Table 2 Antenna Parameters Summary.

Sr. no.	Parameters	Values
1	Frequency (fr)	1800 MHz
2	Radius (R)	0.167 mm
3	Wavelength (λ)	167 mm
4	Dipole Arm (L/2)	39.72 mm
5	Length (L)	79.44 mm
6	Gap (g)	0.3972 mm
7	Matching Impedance (Z0)	50 mm

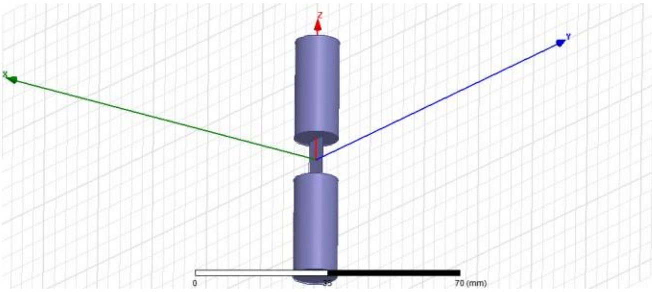

Figure 2 An 1800 MHz HW dipole antenna.

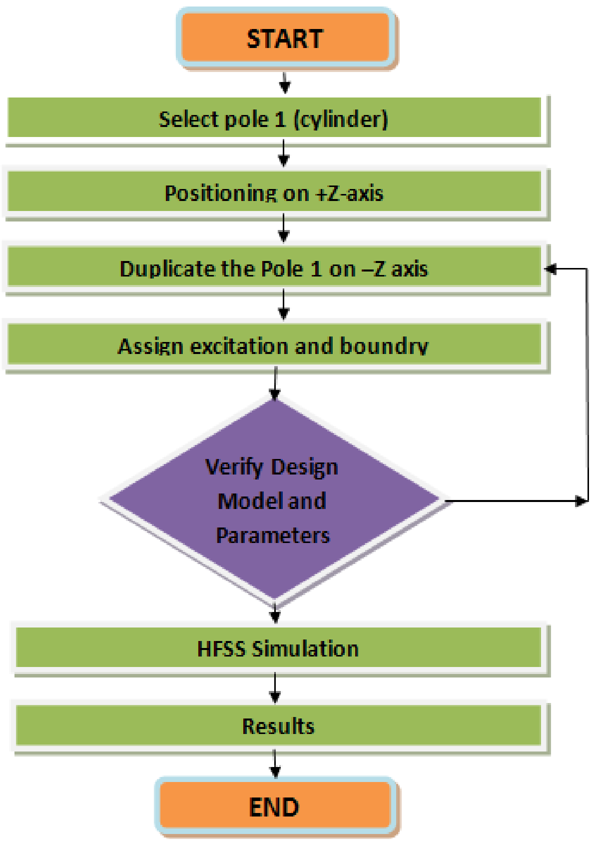

Figure 3 HW Dipole Antenna design Flow Chart for Simulation.

Using the flowchart in Figure 3, an HW dipole antenna simulation was performed.

Figure 4 Bandwidth and return loss curve for an HW dipole antenna.

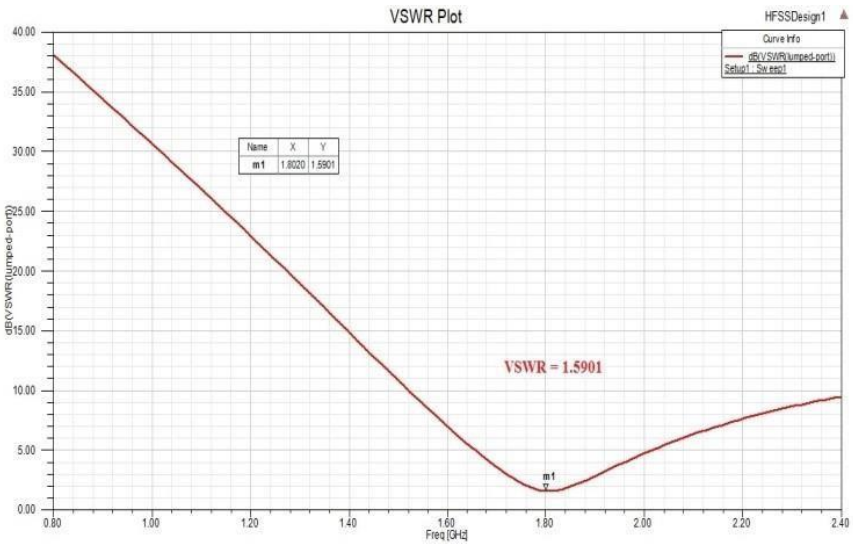

Figure 5 HW dipole antenna VSWR plot.

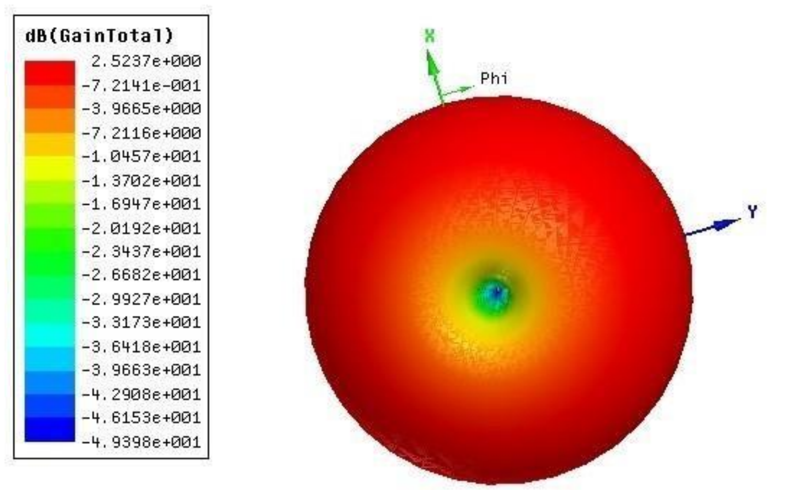

Figure 6 HW dipole antenna 3D gain radiation pattern.

As shown in Figure 4, the proposed HW dipole antenna has a return loss of -20.7710 dB and a bandwidth of 424.3 MHz. The 3D radiation pattern in Fig. 6 and the VSWR, which was 1.5901 dB, both point to a higher gain. In the proposed research work, this HW antenna is utilized as a mobile device model RF radiator.

3.2. Human Head Model

This work has taken into consideration the spherical, multilevel human head model (Abdalla and Teoh 2005). A generalized six-layer tissue model's overall stratified structure may be observed in Figure 7. The thicknesses of the skin, fat, bone, dura, cerebral spinal fluid (CSF), and brain are given as 1.0 mm, 1.4 mm, 4.1 mm, 0.5 mm, 2.0 mm, and 81 mm, respectively (Christ et al 2006). The thickness of the different layers of a head model typically changes with age, gender, and person. The layered media is made up of these elements. The child head geometrical parameters considered 80% of the adult head model (Hadjem et al 2010), as mentioned in Table 3.

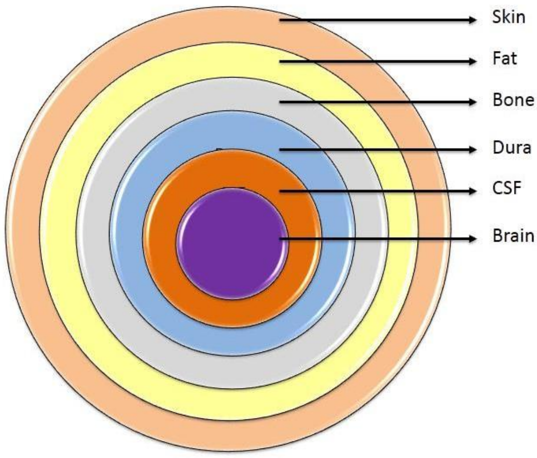

Figure 7 Generalized six-layered model of a human head.

The six-layer head model shown in Figure 8 for the adult head and Figure 9 for the child head model was simulated using the recommended simulation software in accordance with the parameters listed in Table 3.

Table 3 Dielectric properties of adult and child human heads.

Tissue	Permittivity		Conductivity (S/m)		Thickness (mm)	
	Adult	Child	Adult	Child	Adult	Child
Skin	37.21	37.21	1.25	1.28	1.0	0.8
Fat	9.38	9.38	0.26	0.275	1.4	1.12
Bone	16.4	16.4	0.45	0.48	4.1	3.28
Dura	37.21	37.21	1.25	1.28	0.5	0.4
CSF	77.3	77.3	2.55	2.565	2.0	1.6
Brain	43.22	43.22	1.29	1.31	81	64.8

Source: Gabriel and Peyman (2006); Bao et al (1997).

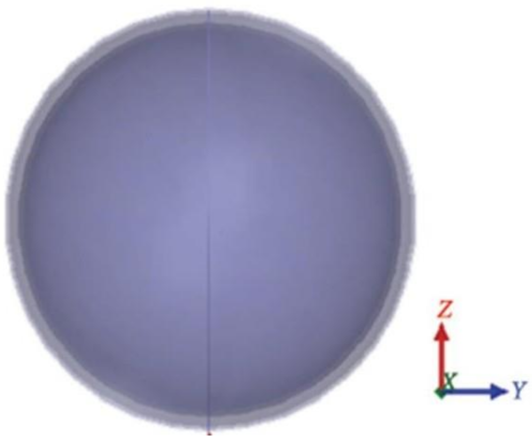

Figure 8 Six-layered Adult Human Head model.

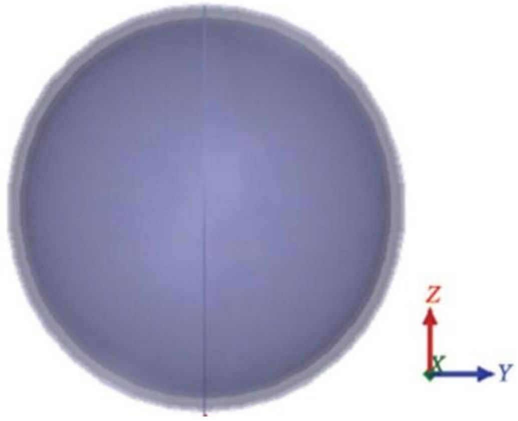

Figure 9 Six-layered Child Human Head model.

4. Simulation for e-field and SAR measurement

4.1. E-field measurement in Adult Head Model

The six-layer adult head model was placed with a powered HW dipole antenna at a 5 mm distance to observe the layerwise e-field and SAR value using the proposed simulation software. Figures 10, 11, 12, 13, 14, and 15 depict the e-field value and SAR value for the skin, fat, bone, dura, CSF, and bone, respectively, in an adult human head. Similarly, the six-layer Child head model was placed with a powered HW dipole antenna at a 5 mm distance to observe the layerwise e-field and SAR value using the proposed simulation software. Figures 16, 17, 18, 19, 20, and 21 depict the e-field value and SAR value for the skin, fat, bone, dura, CSF, and bone, respectively, in a human child head.

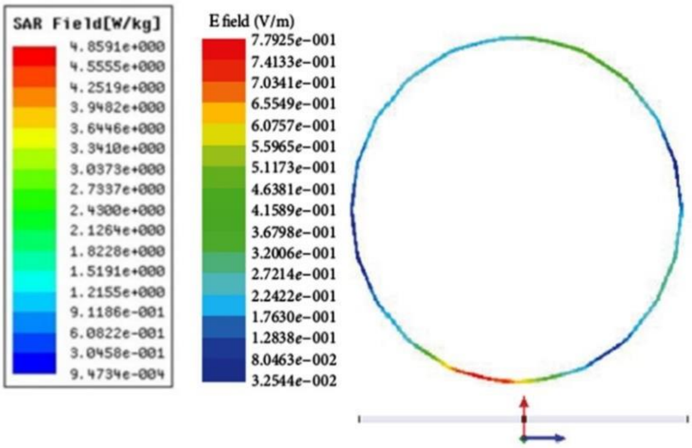

Figure 10 Measurement of the E-field in the adult head skin layer.

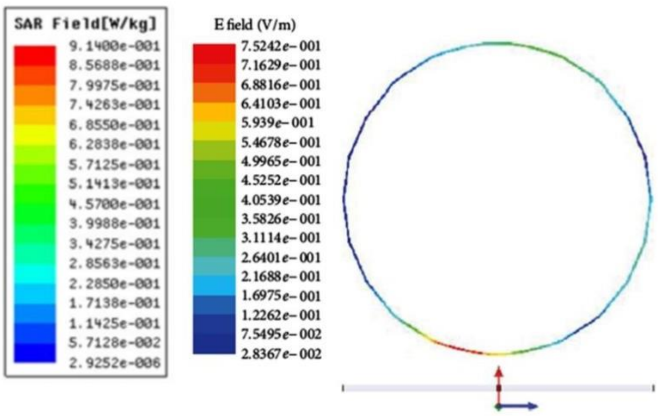

Figure 11 Measurement of the E-field in the fat layer of the adult head.

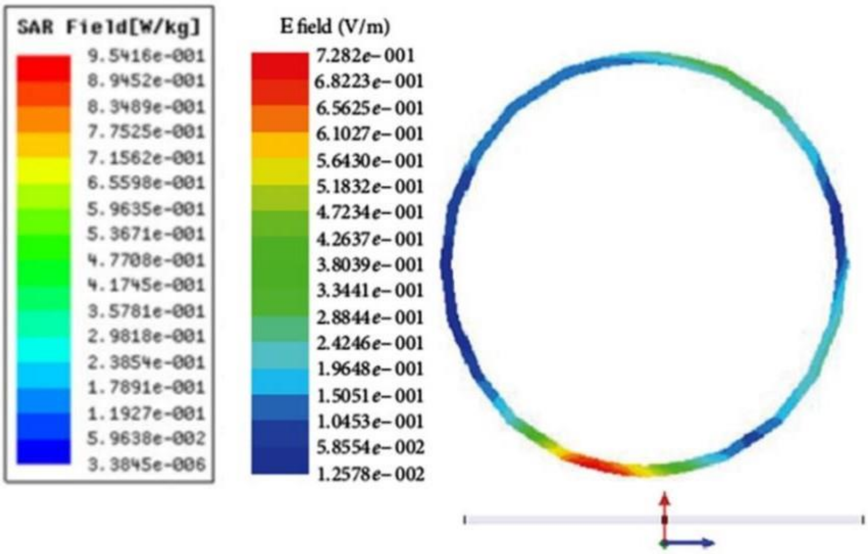

Figure 12 Measurement of the E-field in the bone layer of the adult head.

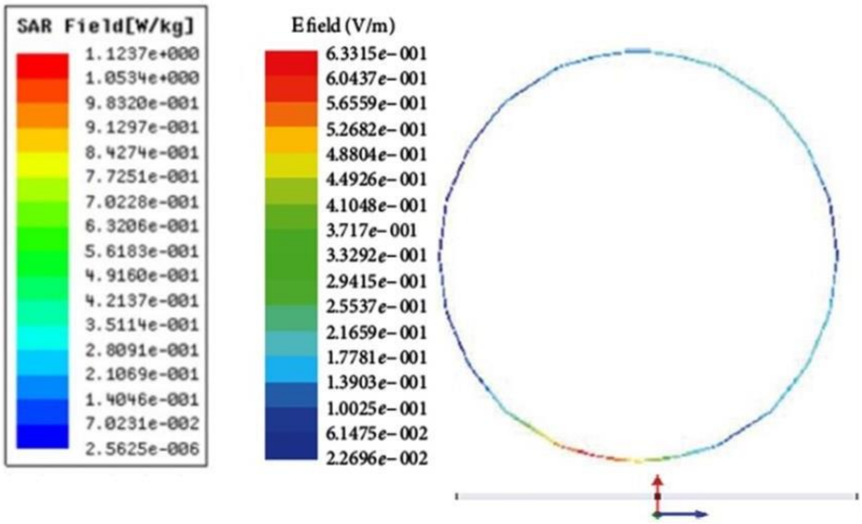

Figure 13 Measurement of the E-field in the dural layer of the adult head.

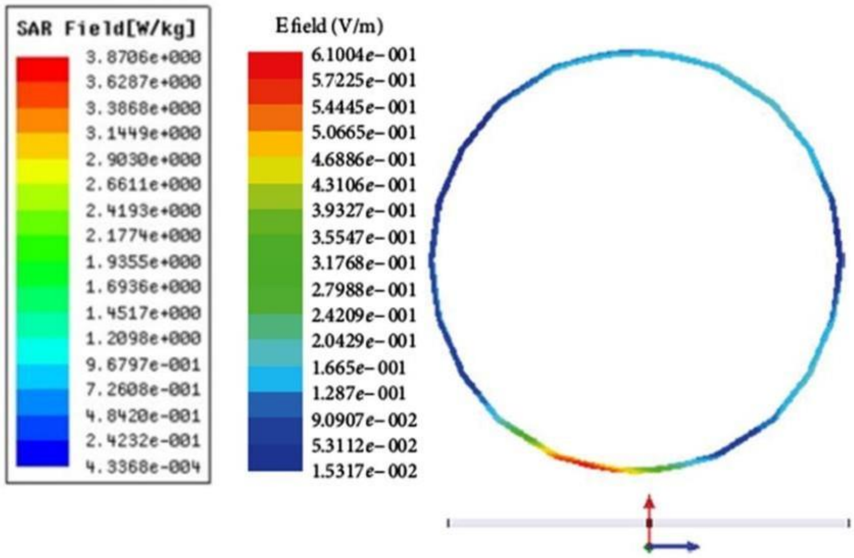

Figure 14 Measurement of the E-field in the CSF layer of the adult head.

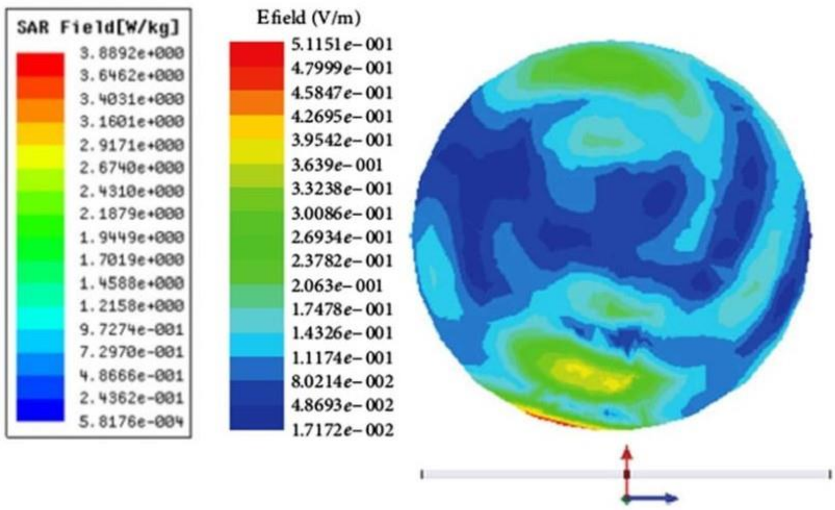

Figure 15 Measurement of the E-field in the brain layer of the adult head.

4.2. E-field measurement in Child Head Model

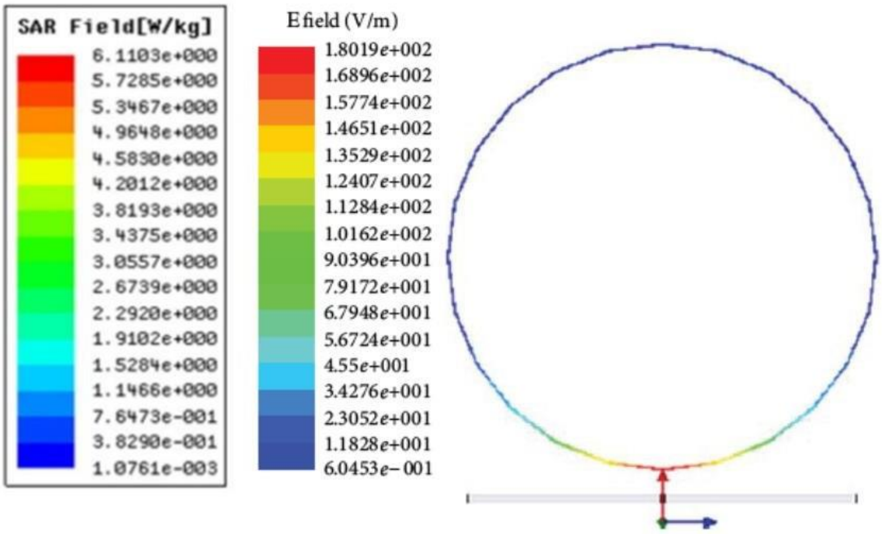

Figure 16 Measurement of the E-field in the child's head skin layer.

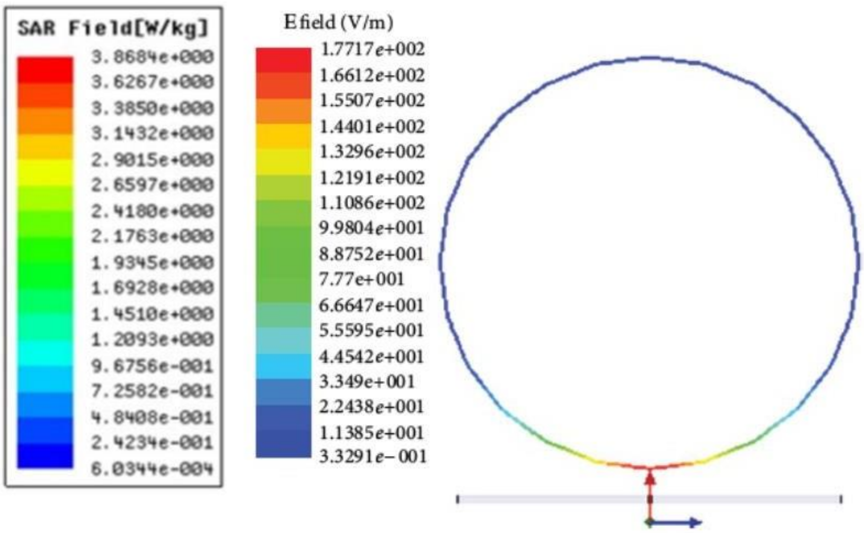

Figure 17 Measurement of the E-field in the fat layer of the child's head.

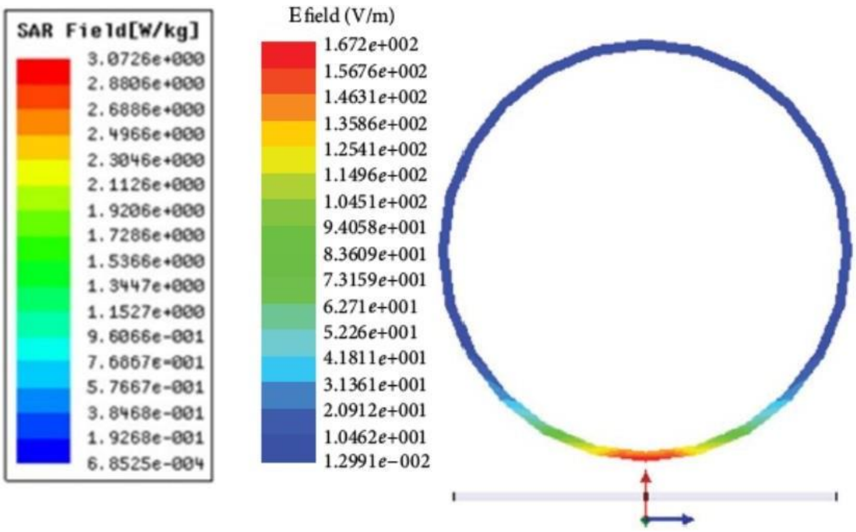

Figure 18 Measurement of the E-field in the bone layer of the child's head.

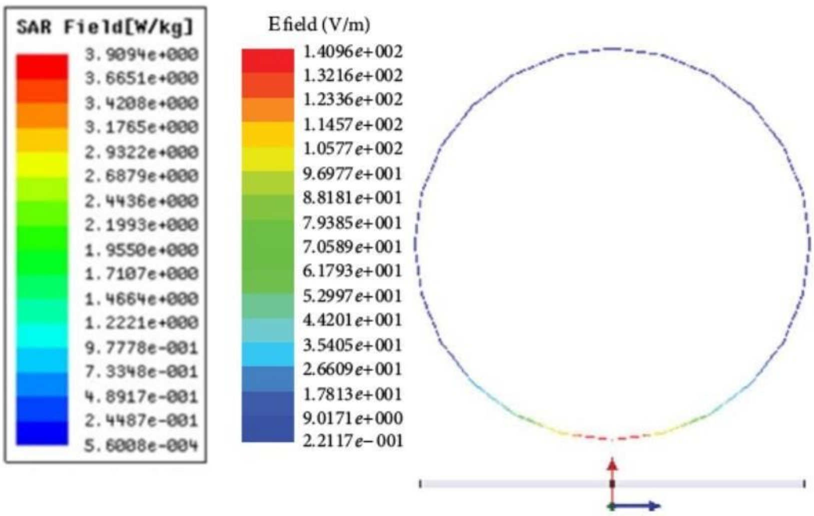

Figure 19 Measurement of the E-field in the dural layer of the child's head.

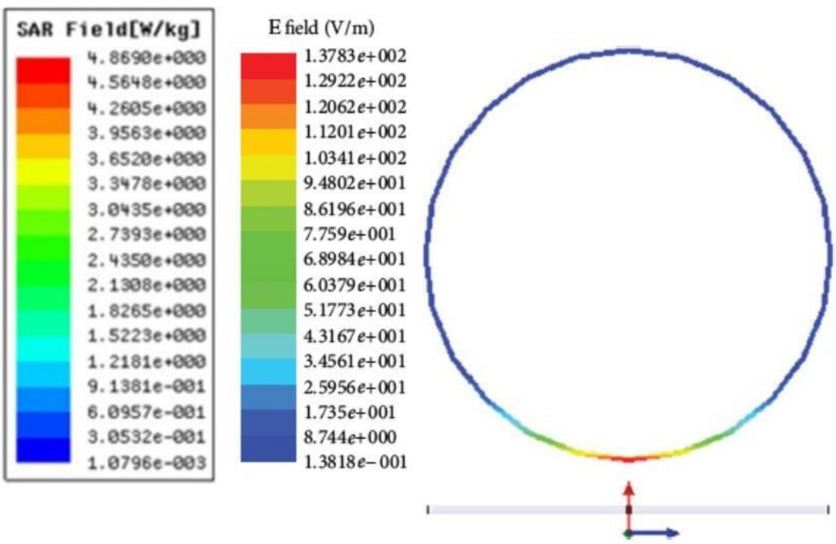

Figure 20 Measurement of the E-field in the CSF layer of the child head.

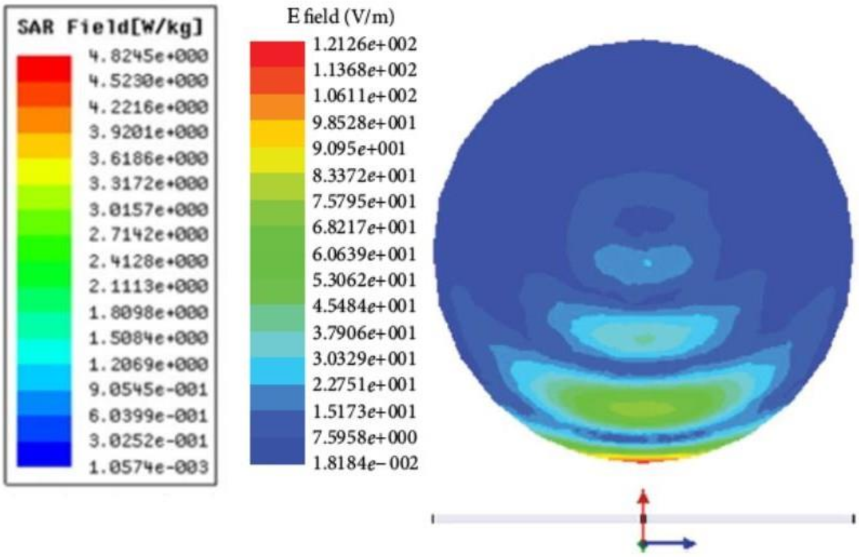

Figure 21 Measurement of the E-field in the brain layer of the child's head.

5. Results and Discussion

Biological tissue displays a dispersive propensity and absorbs power when exposed to electromagnetic radiation. Furthermore, power levels often have a tendency to worsen tissue injury (Davison and Zamah 2009; Bormane et al 2022). Due to the high tissue permittivity, the EM wave absorbs more energy as it reaches the tissue layer at higher frequencies, which causes the tissue to warm up (Wongkasem 2021). In reality, various biological tissues behave like lossy dielectric materials and have a frequency-dependent dielectric constant (Rashed et al 2020). Under adiabatic conditions, tissue heating close to the skin's surface can be significant, whereas the temperature rise in internal body tissues is less noticeable (Christ et al 2006; Sonawane and Bormane 2022). Tables 4 and 5 display the E-field strength and SAR values of the six-layer adult and child human heads.

Table 4 E-field strength of six-layer adult and child human heads.

Sr. No.	Tissue	E-field Strength (V/m) in ADULT Head	E-field strength (V/m) in CHILD Head
1	Skin	0.77925	180
2	Fat	0.75242	177
3	Bone	0.72820	167
4	Dura	0.63315	140
5	CSF	0.61004	137
6	Brain	0.51151	121

Table 5 SAR values of six layers of adult and child human heads.

Sr. No.	Tissue	SAR Value (W/kg) in ADULT Head	SAR Value (W/kg) in CHILD Head
1	Skin	4.85	6.11
2	Fat	0.914	3.86
3	Bone	0.954	3.07
4	Dura	1.12	3.90
5	CSF	3.87	4.86
6	Brain	3.88	4.82

This section analyses the findings of E-field measurements in Table 3 and SAR measurements in Table 4 taken with a dipole using an adult and kid head model for six layers. The geometrical specifications and material dielectric properties for an adult head are different from those for a child's head. A human skull was exposed to the EM produced by a mobile phone (dipole antenna) with a 5 mm distance between it and the electromagnetic source. The frequency band of 1800 MHz was stated in the antenna model design. After examination, an adult head model's maximum E-field and SAR values are 7.7925×10^{-1} volts per metre and 4.85×10^{0} watts per kilogram, respectively. In contrast, the maximum E-field and SAR values for a child head model are $1.80 \times 10^{+2}$ volts per metre and 6.11×10^{0} watts per kilogram, as depicted in Table 3 and Table 4. Figure 22 shows the E-field variance in tissues, and Figure 23 compares the SAR values in human adult and child heads.

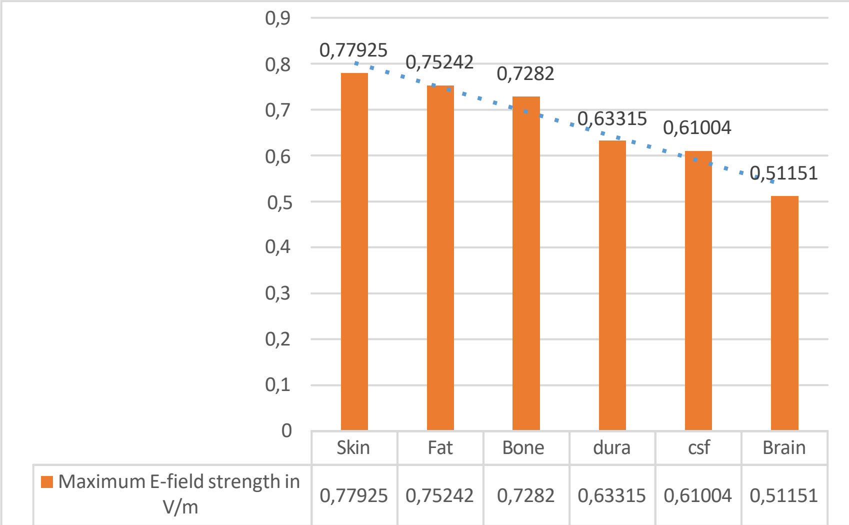

Figure 22 E-field variance in the tissue layer with a change in source distance.

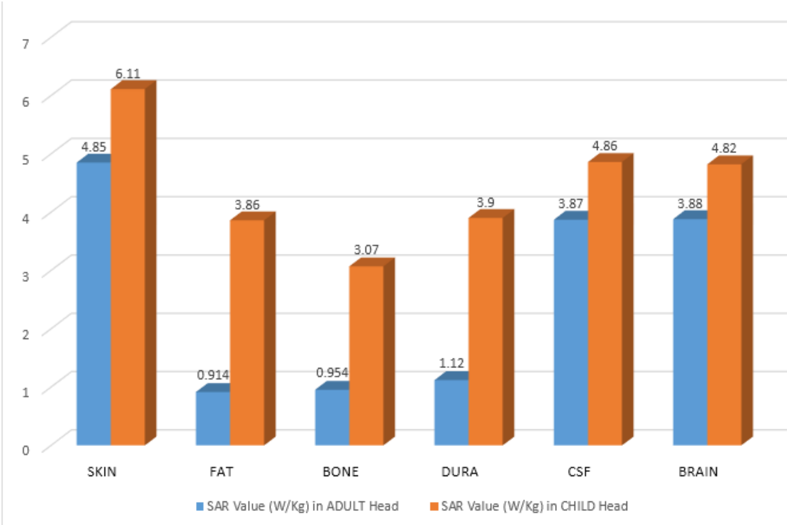

Figure 23 SAR value comparison in human adult and child heads.

The skin layer, which is closest to the EM radiation source, has the highest e-field and SAR value. In both the adult and kid head models, Figure 22 depicts that EM absorption steadily decreases as the distance between the EM source and tissue layer rises, from the skin layer to the brain layer. On comparison, the child head model has a greater SAR than the adult head model, as depicted in Figure 23. Additionally, the bone layer has significantly less water content than other layers, and we found the lowest SAR there. The brain layer, which is the deepest layer, appears to have the second-highest SAR value. SAR changes in six layers of both child and adult heads as a result of layer-by-layer variations in conductivity, permeability, permittivity, and e-field strength.

6. Conclusions

In six-layer (brain, CSF, dura, bone, fat and skin) age-dependent adult and child head models, EM field devices, particularly mobile cell antennae and head contact, have been explored. However, this work places greater attention on the FDTD method age-dependent SAR value measurement approach in 40-year-old adult and 5-year-old child heads. There have been a number of earlier investigations that could have found anatomical differences between adults and children. The scaling of adult head models will always result in certain anatomical variances and sensitivity to EM absorption due to changes in anatomy and tissue proportions.

Due to variations in the pinna's thickness and the cranial bone's thickness, head geometry, conductivity, permittivity and permeability layerwise, the local SAR has been estimated in both scenarios and indicates higher SAR in a child's head than an adult's head. Depending on whether the thickness of the cranium and surrounding tissues genuinely changes with age, a higher SAR in the brains of children can be anticipated. Additionally, the SAR value measured for both adult and child heads surpasses the normal SAR maximum value set by organizations such as IEEE, ICNIRP, and FCC (Means and Chan 2001;

Sonawane and Bormane 2022). According to previous research, using a cellular phone increases the chance of developing brain cancer. That is an ongoing issue. The incidence of glioblastoma, the worst form of brain cancer, has risen in various countries, such as the United States and Denmark (Gabriel and Peyman 2018). In Australia, the frequency of brain cancer has risen recently. These findings are based on data from each nation's cancer registries about brain cancer incidence.

In this study, the strength of e-field absorption in the human head decreases with an increase in the gap between the EM radiator and the head. Therefore, keeping a safe distance from a mobile device could reduce the risk of an unwell effect on the human body/head. If the highest SAR is at or below the 1.6 W/kg exposure level in the United States, the phone is approved for sale without consideration of the SAM certification process's 30% tolerance. However, our research found a larger value than the stipulated limit. Therefore, the safety limitations on SAR for RF exposure must be carefully evaluated for compliance with any wireless devices that may be worn on the body or carried in the hand. The appropriate standards must be changed to account for the effects of electromagnetic field coupling with layered brain tissue. The SAR evaluation results for the two head models may suggest that further standard SAR values should be sought.

7. Future Scope

Due to finding a higher value of SAR in the head of a child, there is a need for a safe solution for the effective design and assessment of EM shields for mobile phones. In the proposed study, the analysis of head SAR has been reported, but body SAR needs to be investigated to determine the severity of the mobile phone effect on the human body.

Acknowledgement

We appreciate and are thankful for the cooperation made by the management, principal and research head of the All India Shri Shivaji Memorial Samsthas Institute of Information Technology (IOIT) to conduct my research in the institute. We also thank and acknowledge my supervisor, who made this work possible.

Ethical considerations

Not applicable.

Conflict of Interest

The authors declare no conflicts of interest.

Funding

This research did not receive any financial support.

References

Abdalla A, Teoh A (2005) A multi layered model of human head irradiated by electromagnetic plane wave of 100 MHz-300 GHz. Int. J. Sci. Res. 15:1-7.

Arima T, Uno T (2012) Whole body SAR measurement technique by using Wheeler cap method for human head size phantom. In 2012 International Symposium on Antennas and Propagation (ISAP), pp. 700–703.

Bao JZ, Lu ST, Hurt WD (1997) Complex dielectric measurements and analysis of brain tissues in the radio and microwave frequencies. IEEE Transactions on Microwave Theory and Techniques 45:1730–1741. DOI: 10.1109/22.641720.

Bormane DS, Kakkeri RB, Kakkeri RB (2022) Surface electromyography signal classification for the detection of temporomandibular joint disorder using spectral mapping method. International Journal of Advanced Computer Science and Applications 13. DOI: 10.14569/IJACSA.2022.0130860.

Christ A, Klingenbock A, Samaras T, Goiceanu C, Kuster N (2006) The dependence of electromagnetic far-field absorption on body tissue composition in the frequency range from 300 MHz to 6 GHz. IEEE Transactions on Microwave Theory and Techniques 54:2188–2195. DOI: 10.1109/TMTT.2006.872789.

Davison JM, Zamah NM (2009) Electrosurgery: Principles, biologic effects and results in female reproductive surgery. The Global Library of Women's Medicine. DOI: 10.3843/GLOWM.10021.

Fernandez-Rodriguez CE, De Salles AAA, Davis DL (2015) Dosimetric simulations of brain absorption of mobile phone radiation–the relationship between pssar and age. IEEE Access 3:2425–2430. DOI:10.1109/ACCESS.2015.2502900.

Gabriel C, Peyman A (2006) Dielectric measurement: Error analysis and assessment of uncertainty. Physics in Medicine and Biology 51:6033–6046. DOI: 10.1088/0031-9155/51/23/006.

Gabriel C, Peyman A (2018) Dielectric properties of biological tissues; variation with age. In Conn's Handbook of Models for Human Aging 939–952. DOI: 10.1016/B978-0-12-811353-0.00069-5.

Hadjem A, Conil E, Gati A, Wong MF, Wiart J (2010) Analysis of power absorbed by children's head as a result of new usages of mobile phone. IEEE Transactions on Electromagnetic Compatibility 52:812–819. DOI: 10.1109/TEMC.2010.2052810.

International Commission on Non-Ionizing Radiation Protection (ICNIRP) (1998) Guidelines for limiting exposure to time-varying electric, magnetic, and electromagnetic fields (up to 300 GHz). International Commission on Non-Ionizing Radiation Protection 74:494–522.

Means D, Chan K (2001) Evaluating Compliance with FCC Guidelines for Human Exposure to Radiofrequency Electromagnetic Fields. Federal Communications Commission Office of Engineering & Technology. Available in: https://transition.fcc.gov/Bureaus/Engineering_Technology/Documents/bulletins/oet65/oet65c.pdf Accessed on: August 2, 2023.

Rashed EA, Diao Y, Hirata A (2020) Learning-based estimation of dielectric properties and tissue density in head models for personalized radio-frequency dosimetry. Physics in Medicine & Biology 65:065001. DOI: 10.1088/1361-6560/ab7308.

Sonawane A, Bormane DS (2022) SAR analysis using a dipole antenna in a non-layered and multi-layered human head model. International Journal on Recent and Innovation Trends in Computing and Communication 10:225–231. DOI: 10.17762/ijritcc.v10i1s.5829.

Sonawane AD, Bormane DS (2020) A specific absorption rate in human head due to mobile phone radiations: Review. International Conference on Electronics and Sustainable Communication Systems (ICESC) 703–707. DOI: 10.1109/ICESC48915.2020.9155777.

Wongkasem N (2021) Electromagnetic pollution alert: Microwave radiation and absorption in human organs and tissues. Electromagnetic Biology and Medicine 40:236–253. DOI: 10.1080/15368378.2021.1874976.